Losses of Soil Organic Carbon with Deforestation in Mangroves of Madagascar

Arias-Ortiz, Ariane; Masque, Pere; Glass, Leah; Benson, Lisa; Kennedy, Hilary; Duarte, Carlos M.; Garcia-Orellana, Jordi; Benitez-Nelson, Claudia R.; Humphries, Marc S.; Ratefinjanahary, Ismael; Ravelonjatovo, Jaona; Lovelock, Catherine E.

Ecosystems

Published: 06/04/2020

Peer reviewed version

This is a post-peer-review, pre-copyedit version of an article published in Ecosystems Journal. The final authenticated version is available online at: https://doi.org/10.1007/s10021-020-00500-z

Losses of soil organic carbon with deforestation in mangroves of Madagascar

Shortened version for page headings: Losses of soil carbon with mangrove deforestation

Ariane Arias-Ortiz[1,2*], Pere Masque[1,3,4,5], Leah Glass[6], Lisa Benson[6,7], Hilary Kennedy[8], Carlos M. Duarte[9], Jordi Garcia-Orellana[1,4], Claudia R. Benitez-Nelson[10], Marc S. Humphries[11], Ismaël Ratefinjanahary[6], Jaona Ravelonjatovo[6], Catherine E. Lovelock[12]

[1]Institut de Ciència i Tecnologia Ambientals, Universitat Autònoma de Barcelona, Bellaterra, 08193 Barcelona, Spain.
[2]Ecosystem Science Division, Department of Environmental Science, Policy and Management, University of California, Berkeley, CA, USA.
[3]School of Science & Centre for Marine Ecosystems Research, Edith Cowan University, Joondalup WA 6027, Australia.
[4]Departament de Física, Universitat Autònoma de Barcelona, Bellaterra, 08193 Barcelona, Spain.
[5]International Atomic Energy, 4a Quai Antoine 1er, 98000, Principality of Monaco, Monaco.
[6]Blue Ventures Conservation, Villa Bella Fiharena, Rue Gambetta, Lot 269, Toliara 601, Madagascar.
[7]Centre for Environment, Fisheries and Aquaculture Science, Lowestoft Laboratory, Lowestoft NR33 OHT, UK.
[8]Ocean Sciences, Bangor University, Menai Bridge, Anglesey LL59 5AB, UK.
[9]King Abdullah University of Science and Technology (KAUST), Red Sea Research Center (RSRC) & Computational Bioscience Research Center (CBRC), Thuwal, 23955-6900, Saudi Arabia.
[10]School of Earth, Ocean & Environment, University of South Carolina, Columbia, South Carolina 29208, USA.
[11]Molecular Sciences Institute, School of Chemistry, University of the Witwatersrand, Johannesburg, South Africa.
[12]School of Biological Sciences, The University of Queensland, St Lucia, QLD 4072, Australia.

*correspondence to aariasortiz@berkeley.edu;

Manuscript highlights:

- Deforestation led to the loss of 20% of 1-m C stocks and increased soil homogeneity
- Annual C loss in deforested soils was 4.5 times the C sequestration of intact soils
- Conservation is temporally more effective than restoration for reducing C emissions

Abstract: Global mangrove deforestation has resulted in substantial CO_2 emissions to the atmosphere, but the extent of emissions from soil organic carbon (C) loss remains difficult to assess. Here, we sampled 5 intact and 5 deforested mangrove plots from Tsimipaika Bay, Madagascar, to examine the loss of soil C in the 10 years since deforestation. We estimated tree biomass and analysed grain size, ^{210}Pb activities, organic C and total nitrogen (N) and their stable isotopes in soils as well as dissolved organic C in surface waters. Deforested soils revealed evidence of disturbance in the upper 14 g cm^{-2} (~ 40 cm) when compared to reference intact soils, indicated by lower porosity, higher dry bulk density, an order of magnitude higher soil mixing and loss of C and N despite no significant soil erosion. While C loss from biomass was unequivocal and was estimated at 130 Mg C ha^{-1}, the C loss from soils was more difficult to assess given the large heterogeneity of intact forest soils. We estimated that the loss of C due to mangrove clearing and soil exposure over 10 years was equivalent to ~ 20% of the upper meter soil C stock, and ~ 45% of the C stock accumulated during the last century. Soil C loss rate was 4.5 times higher than the C sequestration rate in reference intact soils. These results emphasize the importance of mangrove conservation for CO_2 emissions mitigation, as they suggest that deforestation-C losses will take substantially longer to offset with mangrove restoration.

Keywords: Mangroves, deforestation, soil carbon, soil disturbance, CO_2 emissions, Madagascar.

1. Introduction

Mangroves are an important natural resource in the tropics and sub-tropics and provide a wide range of ecosystem services, including coastal protection, support of fisheries and biodiversity, nutrient cycling and carbon sequestration (Barbier and others 2011). Their high rates of primary production and the low rates of organic matter decomposition in their flooded soils lead to mangroves having some of the highest soil organic carbon (C) stocks among forested ecosystems (Donato and others 2011; McLeod and others 2011). However, the C stored in their soils is vulnerable, as mangroves have been widely degraded and converted to alternative land-uses, resulting in losses of ecosystem services (Alongi 2002) and significant carbon dioxide emissions (CO_2) to the atmosphere as previously stored C is remineralized to CO_2 (Lovelock and others 2017b).

Consequences of mangrove soil disturbance include subsidence; as roots die, soil volume collapses and erosion occurs, resulting in loss of soil C. These effects are generally most severe and longer lasting when caused by anthropogenic versus natural perturbations (Ellison and Farnsworth 1996; Twilley and Day 2012). Soil C loss has been observed, for instance, where soils have been excavated for the construction of aquaculture ponds (Ong 1993; Kauffman and others 2014). At sites where mangroves have been removed or uprooted due to human activities or where there have been intense storms, losses of soil C have been inferred from changes in soil elevation (Cahoon and others 2003; Lang'at and others 2014) or measured as CO_2 efflux (Lovelock and others 2011; Sidik and Lovelock 2013; Lang'at and others 2014). Although deforestation has been the major cause of forest loss in the past, there are few studies that have directly measured the change in soil C content in mangrove soils when forests are degraded, but soils remain in place (Kauffman and others 2016; Grellier and others 2017; Adame and others 2018).

A change in soil C content with mangrove deforestation may occur directly as a consequence of biomass loss and/or indirectly due to factors affecting soil biogeochemical processes, such as a change in temperature, physical protection or aeration. For example, variations in mangrove biomass may reduce inputs of labile C and nutrients from detritus, and increased soil temperature from direct sun exposure may result in further loss of soil C (Granek and Ruttenberg 2008). Destructive practices, such as clear cutting, mechanically redistribute C in the soil (Yanai and others 2003; Zummo and Friedland 2011; Lundquist and others 2014), enhancing oxygen diffusion, altering microbial communities and organic C remineralization (Kristensen and Alongi 2006). Physical mixing processes modify the soil structure, transport conditions and soil chemistry, hence potentially changing the availability of C and N for associated microbial and plant communities (Balesdent and others 2000). For instance, the addition of biodegradable C to deep stable C stores promotes microbial respiration of the added and existing organic pools through a priming mechanism (Bianchi 2011), and may accelerate C mineralization beyond that directly derived from mechanical mixing, contributing to elevated CO_2 emissions from soils. Soil C may also be lost as a consequence of soil erosion or exported as dissolved C, a process which may be accelerated through direct exposure of mangrove soils to tidal inundation, rainfall, and waves (Thampanya and others 2006; Labrière and others 2015), as well as through changes in the composition and biomass of benthic mats driven by a reduction in mangrove litter loading (Delgado and others 1991; Duke and Wolanski 2001; McKee 2011; Grellier and others 2017).

Overall, soil C storage represents a balance of C inputs and losses, and because soil is the largest reservoir of C in many mangrove ecosystems (Donato and others 2011), small changes in its pool size may translate into significant CO_2 emissions and changes of C fluxes to coastal waters (Atwood and others 2017; Gillis and others 2017). While it is well established that the harvesting of terrestrial forests results in a loss of C in organic and mineral soil horizons (Yanai and others 2003;

Diochon and others 2009; Zummo and Friedland 2011), the impact of mangrove deforestation on soil C storage remains limited. Direct assessment of these C losses is important for quantifying CO_2 emissions from mangrove deforestation and in the value associated with avoiding emissions achieved through conservation projects (Herr and others 2017). Currently, guidance by the International Panel for Climate Change on CO_2 emission from coastal wetlands (IPCC 2014) has a "*tier 1*" (i.e., default) assumption that soil CO_2 emissions and removals are zero for forest management practices in mangroves. However, the IPCC allows for country-specific "*tier 2*" (i.e., based on direct assessments) to be adopted by using a C stock-difference method in order to account for any emissions associated with forest management practices.

In this study we aim to quantify the C loss from deforested mangrove soils in northwest Madagascar. Madagascar contains Africa's fourth largest national extent of mangroves, representing approximately 2% of the global mangrove area. Since 1990, more than 20% of Madagascar's mangrove ecosystems have been heavily deforested because of the increasing demand for charcoal and timber by urban populations (Jones and others 2016a), which is the primary cause of mangrove deforestation in the broader East African region (FAO [Food and Agriculture Organization of the United Nations] 2007). We sampled soil cores from plots that were either within deforested and intact forest areas to assess the change of soil C after clearing. We described the physical characteristics of soils with depth, quantified the variation in C and N contents, and estimated sediment accumulation rates, soil mixing and potential erosion using the natural radionuclide lead-210 (^{210}Pb) ($T_{1/2}$: 22.3 yr) (Appleby 2001; Arias-Ortiz and others 2018). We also measured dissolved organic C (DOC) in adjacent coastal surface waters to assess the effects of deforestation on DOC export 10 y later. Finally, we use our data to estimate the fate and total change of soil C since mangrove clearance.

2. Methods

2.1 Study site

This study was conducted in Tsimipaika Bay (previously referred to as Ambanja Bay; Jones and others 2016a) in northwest Madagascar (48°28'E, 13°30'S), where anthropogenic mangrove loss is particularly prominent due to extensive extraction for charcoal and timber (Jones and others 2014). Together with Ambaro Bay, the Tsimipaika-Ambaro Bay complex forms Madagascar's second most extensive mangrove ecosystem, with over 40,000 ha of mangrove forests (Jones and others 2014, 2016a). The site is characterized by a humid sub-tropical climate and is influenced by semi-diurnal tidal ranges varying between maximums of 3.0 – 3.5 m (Rasolofo and Ramilijaona 2009). Mangrove soils in this region are underlain by alluvial and lake deposits (Jones and others 2016b) flooded by sea level rise. Contemporary localized mapping supported by field observations indicated that, in 2010, anthropogenic activities had driven substantial deforestation (1,000 ha) mostly near the southwest region of the peninsula that separates the two bays (Jones and others 2014) (Fig. 1). Deforestation heavily targets closed canopy mangrove forests followed by open canopy mangroves (Benson and others 2017), which represent 30 and 56% of the total mangrove area at the Tsimipaika-Ambaro Bay complex, respectively (Jones and others 2014). *Rhizophora mucronata* is favored for the charcoal production process, in which trees are felled by hand and carried to nearby temporary kilns to be carbonized. Non-*Rhizophora* species and unwanted prop roots are burned to heat kilns, although large volumes of downed wood are often discarded at the site.

In November 2016, we sampled soil cores from 5 plots that were cleared between 2006 and 2008 and from 5 plots from an intact forest (Fig. 1). The deforested and forested plots were spatially separated by ~5 km but had relatively similar environmental conditions such as species composition, hydroperiod, type and proximity of bedrock and nutrient inputs. Within the sampled plots, four species of mangroves were present: *Rhizophora mucronata, Bruguiera gymnorhiza, Ceriops tagal* and *Sonneratia alba* (Table 1). Intact plots were all well-formed, closed (> 60%) canopy mangroves,

consisting of high stature trees (mean height: 9.0 ± 0.5 m) of variable density (800 - 4,700 ha^{-1}). The average diameter at breast height (1.3 m, dbh) was 12 ± 2 cm. Deforested plots used to contain closed canopy mangrove forests (Blue Ventures, personal communication) and this was evident from plots comprised of *Ceriops tagal* or *Bruguiera gymnorhiza* where the boles left in place after tree removal lead to stump densities ranging from 1,000 to 11,400 ha^{-1} (Table 1).

Aboveground tree biomass at each plot (Table S1) was derived from tree diameter and height measurements using generalized species-specific allometric equations (Clough and Scott 1989; Cole and others 1999; Chave and others 2005; Kauffman and Donato 2012) and wood density values (Chave and others 2009; Zanne and others 2009). These equations were chosen based on the region in which they were developed and the parameters used to derive them, and have been previously described in Jones and others (2016b) for use in the same area. The maximum tree diameter and height measured (18 cm and 10 m, respectively) were within the range of trees used to develop the equations. Tree belowground-biomass was calculated using the generalized equation presented in Komiyama and others (2005) and equations from Kauffman and Donato (2012) were used to estimate the biomass of standing dead wood. From biomass density estimates, the total biomass C stocks (Mg C ha^{-1}) were estimated using conversion factors of 0.50 and 0.39 for above and belowground estimates, respectively (Kauffman and Donato 2012), and should therefore be considered as approximate estimates of biomass C. Plot size for tree measurements was 100 m^2 and estimates of biomass and C stocks were scaled to the hectare-level.

2.2 Sampling and analytical methods

In order to characterize soil biogeochemical properties, PVC tubes (1.5 m long, 6.2 cm inner diameter) were hammered into mangrove soils (one at each plot; Fig 1), extracted by hand and transported to the laboratory. Prior to extracting the core, the depth to the sediment surface inside and

outside the core was measured in order to assess core shortening during sampling (Glew and others 2001), which averaged 36 ± 10% and 50 ± 13% in intact and deforested mangrove soils, respectively. The PVC corers were cut lengthwise, and the soils inside the corers were sliced at 0.5 cm-thick intervals throughout the first 20 cm, and at 1 cm-thick intervals below this depth. Soil depth layers were weighed wet and then dried at 60ºC until a constant weight was achieved. Soil water content and dry bulk density (DBD) were then calculated. Soil mass per unit area (g cm^{-2}) was also estimated at each layer by dividing the dry sample mass by the core tube area sampled. The lack of a reference elevation marker in sampled intact and deforested soils made comparisons of soil properties based upon depth or volume limited and less precise (Gifford and Roderick 2003; Wendt and Hauser 2013). We thus used the cumulative mass approach. The cumulative soil mass of each core was calculated by summing their respective soil mass layers to the bottom of the core. Soil profiles were displayed in terms of cumulative mass rather than depth to accommodate the impact of changes in the DBD, and thus surface elevation change, which may occur through soil collapse after deforestation (Cahoon and others 2003; Krauss and others 2010; Lang'at and others 2014), the influence of trampling (Kauffman and others 2004), swelling and shrinking with changes in moisture content (Haines 1923) and due to variable soil shortening and compaction during coring.

Soil C and total nitrogen (subsequently notated as N) contents were measured at 1 cm resolution throughout the upper 30 cm, and in alternate slices every 5 cm below this depth. Prior to analysis, soil samples were sieved (1.5 mm) to exclude belowground biomass before being ground to a fine powder. Sub-samples (~ 20 mg) were weighed into silver cups, acidified with 1 M HCl, dried at 60ºC and then analysed using an elemental analyser (Carlo Erba NA1500). No visual evidence of effervescence was observed during sample acidification, which indicates that minimal inorganic C was present. Analytical precision (s.d. of n = 26) was ± 0.3% for C, ± 0.02% for N and ± 4 for molar C:N ratios. Stable isotopes of sediment C and N ($\delta^{13}C$ and $\delta^{15}N$) were analyzed at one core per treatment location using an elemental analyzer–isotope ratio mass spectrometer (Hilo Analytical

Laboratory) at the University of Hawaii. Sub-samples for stable isotope analyses were encapsulated in silver cups and acidified as described above. The use of a weak 1 M HCl solution was chosen following the recommendations in Kennedy and others (2005). Replicate and control samples (NIST 8704) were also run and the accuracy and precision of $\delta^{13}C$ and $\delta^{15}N$ data were of ± 0.2‰ and ± 0.07‰, respectively.

Grain size analyses were conducted down core to evaluate potential erosion, which results in selective and preferential loss of smaller size grain fractions (Arata and others 2016). Sediment grain-size was measured with a Mastersizer 2000 laser diffraction particle analyzer following digestion of bulk samples with hydrogen peroxide to remove organic matter. Sediments were classified as sand (63 - 1,000 μm), silt (4 - 63 μm) and clay (< 4 μm) (size scale: Wentworth 1922).

Specific activities of ^{210}Pb were measured down core in order to assess soil accumulation rates and soil erosion. Total ^{210}Pb was determined through the analysis of its granddaughter ^{210}Po by alpha spectrometry after complete sample digestion in a HNO_3:HF mixture (9:3 ml) using an analytical microwave in the presence of a known amount of ^{209}Po added as a tracer (Sanchez-Cabeza and others 1998). Certified reference materials IAEA-447 and IAEA-385 were analyzed alongside soil samples. Accuracy of the ^{210}Pb(^{210}Po) measurements averaged 96 ± 4%. The specific activities of $^{210}Pb_{xs}$ used to obtain the age models were determined as the difference between total ^{210}Pb and ^{226}Ra (supported ^{210}Pb). Specific activities of ^{226}Ra were determined for selected samples within each core by gamma-spectrometry through the measurement of ^{226}Ra decay product emission lines of ^{214}Pb at 295 and 352 keV and using calibrated geometries in a HPGe detector (CANBERRA, Mod. SAGe Well). Total ^{210}Pb activities at depth derived by alpha and ^{226}Ra specific activities via gamma were within error of one another confirming agreement between alpha and gamma methods. Mean sediment accumulation rates over the last several decades to century were estimated for intact mangrove soils using the Constant Flux:Constant Sedimentation (CF:CS) model applied below the surface mixed layer (Krishnaswamy and others 1971) following the recommendations in Arias-Ortiz

and others (2018). Mass accumulation rates (MAR) are expressed in cumulative dry mass units (g cm^{-2} y^{-1}) and accretion rates (SAR) in mm y^{-1}. Carbon accumulation rates (CAR) were estimated as the product of the fraction of %C accumulated down to the excess ^{210}Pb horizon (C_t) by the MAR of that period (MAR_t):

$$CAR = C_t \cdot MAR_t \quad \text{(Eq.1)}$$

The same equation can be applied to estimate N accumulation rates. Potential soil erosion triggered by mangrove removal was assessed by comparing the $^{210}Pb_{xs}$ inventories ($^{210}Pb_{xs}$ activity per unit area) at deforested mangrove soils against the inventories measured in intact mangrove soils.

Soil C stocks were quantified using equivalent soil mass layers rather than depth to account for variations in bulk density across sites and down core. The soil mass layers used as the basis for comparison were 14 g cm^{-2} (upper), which represented soils accumulated in the last century (based on the average $^{210}Pb_{xs}$ horizon), 14 - 45 g cm^{-2} (bottom), and 45 g cm^{-2} (total), which was the average cumulative mass equivalent to approximately 1 m of soil. Estimates of soil C stocks integrated to a depth of 1 m are also reported for comparison to global estimates. For the latter purpose, we corrected soil depth for core shortening by linearly distributing the spatial discordance between the length of the recovered soil and the depth penetrated by the core tube to the sliced soil layers following Morton and White (1997). We acknowledge that by using a whole-core value, differential interval shortening with depth might be underestimated and could lead to erroneous conclusions regarding the magnitude of deformation and the need for depth corrections. Here, cumulative mass intervals were used as a reference for detailed depth-dependent quantitative comparisons. A different coring method that reduces shortening (Hargis and Twilley 1994) or the taking of several intermittent measurements of soil shortening during coring (Morton and White 1997) would have been necessary to use depth-based approaches.

Surface water samples were collected over a tidal cycle at 8 sites along the shore adjacent to the intact (stations 1-4) and deforested (stations 5-8) mangrove areas. The intact sites were sampled

during the flood to high slack tide. The deforested sites were sampled during the ebb to low slack tide. Samples for total organic C were collected in 20 mL combusted glass vials, acidified to pH of 2 and stored at 4°C until analysis. Samples were analyzed as both filtered (using acid-washed and pre-combusted syringe GF/F filters) and unfiltered samples. Total and dissolved organic C were measured using high temperature (720°C) catalytic oxidation (Pt-alumina) on a Shimadzu TOC-V CPN analyzer (Benner and Strom 1993). Analytical replication (5 injections, 100 μL) of consensus reference material (Florida Straight at 700 m, DOC-CRM program) was run every 10 samples. High concentrations were also measured diluted with distilled and deionized water. Total organic C versus filtered DOC concentrations, and high concentration versus diluted samples were found to be the same within error (± 50 μmol C L^{-1}).

2.3 Statistics

Water content, DBD, C and N content and molar C:N ratios in soils as well as DOC concentrations in surface waters were not normally distributed, and thus non-parametric tests were used to assess significant differences between intact and deforested areas (Mann-Whitney test) at a level of significance of < 0.05. We used principal component analysis (PCA) to assess the relationship between soil properties and the two areas studied (intact and deforested mangroves). Sediment grain size, $^{210}Pb_{xs}$ inventories, $\delta^{13}C$ and $\delta^{15}N$, and stocks did follow a normal distribution, hence a two-sample t-test was used to assess significant differences between intact and deforested mangrove soils. Mean ± SE values are reported throughout the manuscript together with median values where variables were not normally distributed.

2.4 Emissions from mangrove forest deforestation

We analysed C losses and potential emissions from mangrove deforestation based upon the variation in C content in the mangrove soil profiles between intact and deforested soils. Likewise,

biomass C loss was estimated as the difference between vegetation C stocks in intact and deforested plots. The losses of C were reported as CO_2 equivalents (CO_2e), obtained by multiplying C loss values by 3.67, i.e., the molecular ratio of CO_2 to C. The mean annual rate of C loss from deforested soils was estimated as the total soil C stock loss divided by the time elapsed since disturbance (10 years).

3. Results

The effect of deforestation was obvious due to differences in mangrove vegetation compared to undisturbed sites. Total estimated biomass C stocks in intact plots ranged from 113 to 254 Mg C ha^{-1}, while in deforested plots these were substantially lower (0.06 to 9.5 Mg C ha^{-1}) and contained negligible belowground biomass (i.e., roots) (Table 1 and Table S1). The effects of deforestation were less clear in soils from deforested mangroves, which contained similar average C and N contents to intact mangroves over the total soil profile ($P > 0.05$) (Table 2). This was in part because variability in soil properties within the five intact mangrove cores was large and data followed a bimodal distribution (Fig. S1). Intact soils Cc19 and Cc20, hereafter referred to as high-DBD intact soils, were depleted in water content and had significantly higher soil DBD and lower C and N contents relative to deforested soils ($P < 0.01$). In contrast, intact plots Cc18, Cc28 and Cc29, hereafter referred to as low-DBD intact soils, had significantly lower DBD and higher water, C and N contents than deforested soils ($P < 0.01$). As a consequence, physico-chemical properties of deforested soils fell between those of high-DBD and low-DBD intact soils (Table 2).

Multivariate analyses further confirmed that soils from intact mangroves were represented by two clusters of data and that deforested soils were comparable to a mixture of low- and high-DBD intact soils, with characteristics closer to low-DBD intact soils (Fig. 2). Principal components Pc1 and Pc2 explained 75% of the total variance among sampled soils. Pc1 comprised 50% of the variance and was strongly correlated with soil DBD ($r = -0.90$), water, and C and N contents ($r =$

297 *0.95, r = 0.95* and *r = 0.94*, respectively). Pc2 explained 25% of the variance and was strongly
298 correlated with clay (r = 0.91) and moderately correlated with C:N ratios (*r = 0.53*).
299
300 Concentrations of DOC in surface ocean waters varied widely between stations, with 8 times
301 higher median concentrations measured during ebb tide (Fig. 3). Stations 1- 3, adjacent to the intact
302 mangrove area and sampled during the flood tide, had the lowest DOC concentrations (320 ± 30
303 μmol C L^{-1}) contrasting with those measured at station 4 (3,500 ± 50 μmol C L^{-1}), also adjacent to
304 the intact forest, but sampled during the high slack to ebb tide. All surface waters nearshore of the
305 deforested mangroves were sampled during the ebb to low slack tide, leading to some of the highest
306 DOC concentrations, ranging between 1,000 and 19,400 μmol C L^{-1}. Due to tidally-driven
307 variability, no significant differences could be observed in median surface water DOC concentrations
308 between intact and deforested nearshore areas (*P = 0.19*).
309
310 **3.1 Soil physico-chemical properties downcore**
311 Changes in soil physico-chemical properties over the soil profile were observed in low-DBD
312 intact and deforested mangrove soils only. In soils from low-DBD intact mangroves, DBD increased
313 linearly and water content decreased with soil cumulative mass (or depth in g cm^{-2}, hereafter).
314 Deforested soils, however, displayed a constant and significantly higher DBD, with decreasing water
315 content over the upper 14 g cm^{-2} (or ~ 40 cm) (*P< 0.01*; Table S2) (Fig. 4a and b).
316
317 Carbon and N content (%DW) in low-DBD intact mangrove soils decreased steadily
318 downcore, opposite to the pattern observed in deforested soils, which increased with depth in the
319 upper 14 g cm^{-2} (Fig. 4c and d). The mean soil C content of low-DBD intact soils was 8.4 ± 0.2% C
320 in the upper 14 g cm^{-2}, 2-fold higher than that in deforested soils (4.7 ± 0.2% C). Below this horizon,
321 however, no significant differences were observed in water, C or N contents between deforested and

low-DBD intact soils (Fig. 4) (Table S2). In contrast, soil properties of high-DBD intact soils remained relatively constant and differed significantly from those in low-DBD intact and deforested soils throughout the soil profile (Table 2).

Molar C:N ratios were high in all sampled soils with averages ranging from 29 to 33, and increased downcore in low-DBD intact and deforested soils. Correlation between C:N ratios and soil cumulative mass was positive and significant in all treatments ($P < 0.001$) except for the high-DBD intact soils ($P > 0.05$). The relationship was strongest in the upper 14 g cm^2 of deforested soils (r_s = 0.54) and the slope higher than in the low-DBD intact soils (r_s = 0.41) (Fig. S2). Although, deforested soils were characterized by higher average C:N molar ratios over the total soil profile no significant differences were observed in bottom layers between low-DBD intact and deforested soils (Table S2).

Stable isotopes of C and N were analysed for one low-DBD intact and one deforested soil. Both mangrove soils showed $\delta^{13}C$ values close to -28‰ although C in the deforested soil had lighter average $\delta^{13}C$ values (-28.16 ± 0.05‰) than C in the intact soil (-27.5 ± 0.1‰) ($P < 0.001$). In contrast, the $\delta^{15}N$ signal averaged 0.92 ± 0.10‰ and was not significantly different between the two soil types ($P = 0.70$). Soil C in low-DBD intact soil showed $\delta^{13}C$ values that became slightly heavier (+1.2‰) over the upper layer and relatively constant in the bottom layer (Fig. 4c). The deforested soil showed an initial change from heavy to lighter $\delta^{13}C$ values at ~ 3 g cm^{-2} before becoming heavier downcore (Fig. 4d). $\delta^{15}N$ showed a similar pattern as $\delta^{13}C$ in the intact soil but showed scattered values down core in the deforested soil.

The grain size distribution of all intact and deforested mangrove soils was relatively homogeneous over the soil profile. Silt accounted for 52 ± 5% and 58 ± 6% of dry weight, respectively. However, the average clay content (< 4 μm) in deforested soils (28 ± 1%) was about twice that of high-DBD (11 ± 1%) and low- DBD intact soils (15 ± 1%) (Fig. S3). No significant

differences in clay content were observed with depth in any of the sampled soils (*P > 0.01*; Table S2).

3.2 ^{210}Pb

In all intact mangrove soils, the excess ^{210}Pb ($^{210}Pb_{xs}$) specific activity decreased from the surface to below detection at depths between 7 and 17 g cm^{-2} (Fig. 5a). The CF:CS model was used to estimate average mass accumulation rates over this depth horizon (Krishnaswamy and others 1971), which ranged between 0.070 ± 0.014 g cm^{-2} y^{-1} and 0.223 ± 0.012 g cm^{-2} y^{-1} (or 0.85 ± 0.11 and 8.4 ± 0.4 mm y^{-1}; Table 3) at intact sites. In deforested mangrove soils, $^{210}Pb_{xs}$ horizons were reached at 10 to 26 g cm^{-2} (18 ± 3 g cm^{-2}) but intense soil mixing, indicated by uniform specific activities of $^{210}Pb_{xs}$ throughout deforested soil profiles, precluded the determination of a valid age model and sediment accumulation rates at these sites. Indeed, the cumulative mass of the soil mixed layer was on average 10 times greater in deforested than in intact soils (14 g cm^{-2} versus 1.4 g cm^{-2}) (Table 3). The $^{210}Pb_{xs}$ inventories in intact mangrove soils varied widely (600 - 4,800 Bq m^{-2}), although the average (2,210 ± 800 Bq m^{-2}) was not significantly different to that observed in deforested mangrove soils (mean 1,930 ± 220 Bq m^{-2}) (P = 0.74), where the $^{210}Pb_{xs}$ inventory was redistributed over the soil profile via mixing. It should be noted that high-DBD intact soils contained the lowest $^{210}Pb_{xs}$ inventories (600 ± 100 Bq m^{-2}). This could potentially mask significant differences between intact and deforested $^{210}Pb_{xs}$ inventories, and therefore, erosion patterns using the targeted inventory comparison. However, the mean $^{210}Pb_{xs}$ inventory of low-DBD intact soils was also not significantly different than that of deforested soils (P = 0.08), indicating the lack of erosion at deforested sites relative to reference intact sites.

3.3 C and N accumulation rates and stocks

Mean soil C and N burial rates during the last century within the closed canopy forest ranged from 18 to 176 g C m^{-2} y^{-1} and from 0.7 to 7.2 g N m^{-2} y^{-1}, respectively, not including belowground biomass accumulation. In low-DBD intact soils, C and N burial rates averaged 110 ± 40 g C m^{-2} y^{-1} and 4 ± 2 g N m^{-2} y^{-1}, respectively and were similar to burial rates estimated globally (Breithaupt and others 2012) but 5 times higher than those found in high-DBD intact soils (Table 4). In deforested plots, soil C and N burial rates could not be estimated due to soil mixing over the entire $^{210}Pb_{xs}$ record.

Evidence for soil C and N losses was clear between deforested and low-DBD intact soils in the upper 14 g cm^{-2}, which encompasses soils accumulated during the last century, as indicated by the average depth of $^{210}Pb_{xs}$ horizon in all sampled soils (Table 3). Over this depth and equivalent period of accumulation, stocks of C and N in deforested soils were half those of low-DBD intact soils (Table 4). No significant differences, however, were observed if high-DBD intact soils were included in the comparison or if stock comparisons were made over the upper 45 g cm^{-2} or 1 m of soil ($P > 0.05$ in all cases).

4. Discussion

Changes in soil C stocks following deforestation can be an important component of the ecosystem C budget and therefore climate mitigation. This is particularly true for ecosystems such as mangrove forests. In Madagascar, clearing and harvesting of the mangrove forest between 1990 and 2010 has resulted in an estimated net loss of ~ 21% of mangrove cover (Jones and others 2016a), but the effects of these activities on soil C storage are poorly known. Carbon losses from soils following mangrove clearance are more difficult to assess than aboveground stocks. The slow rate at which soil C stocks change and their inherently large spatial variability make quantification of recent changes unclear, especially when soils have remained on site but have been mixed and/or compacted and

reference soil depths are no longer valid. As evidenced from the low- and high-DBD intact mangrove soils in this study and reported elsewhere (Chmura and others 2003; Ferreira and others 2010; Kauffman and others 2014; Otero and others 2017), intact mangrove soils are heterogeneous. Soil heterogeneity can be increased by mangroves themselves through biotic processes such as colonization, root activity and distribution, and decomposition (Boto and Wellington 1984). It can also occur from environmental processes such as coastal evolution and changes in creek configuration (Macnae 1969; Semeniuk 1996; Ferreira and others 2010), differences in tidal water flooding or sediment supply (Chmura and others 2003). We observed a wide range and variability in soil physico-chemical properties and C and N stocks and accumulation rates in soils from intact mangroves in Tsimipaika Bay that were independent of aboveground biomass, mangrove species or distance from shore, but showed a 5-fold difference in soil accretion rates between soils in high- and low-DBD intact mangrove plots. In contrast, soil properties including $^{210}Pb_{xs}$ inventories and C and N profiles appeared spatially homogeneous among cleared soils, suggesting that deforestation and the continuous exposure of soils caused a general loss of natural variability. This pattern was also reported by Stoke and Harris (2015) in New Zealand and, although often overlooked, may be an additional sign of ecosystem function and service loss (Stover and Henry 2018).

The effects of deforestation and the continuous exposure of soils over 10 years were clear in the upper 14 g cm^{-2} (or apparent ~40 cm). Over this depth, all deforested soils showed evidence of disturbance as indicated by lower water content, higher DBD, 10-times higher soil mixing and a higher depletion of C and N contents at the surface. Pre-existing soil properties and C and N stocks were unknown at deforested plots. However, the strong convergence of soil properties between deforested and low-DBD intact soils below 14 g cm^{-2} (Fig. 4; Table S2) allowed us to use the latter as a reference for pre-deforestation conditions. This approach has been used previously (Grellier and others 2017), and gives first-order estimates of biomass and soil C and N loss. Both low-DBD intact and deforested soils showed isotopic $\delta^{13}C$ values of sedimentary organic C similar to those of

mangrove vegetation (-29.4 to -27‰; Bouillon and others 2008b) suggesting that the source of organic matter was predominantly of mangrove origin at both sites. The enrichment of $\delta^{13}C$ and $\delta^{15}N$ with depth in low-DBD intact soils was consistent with organic matter decomposition with age (Fourqurean and Schrlau 2003) and with the Suess effect, i.e., the temporal decrease in atmospheric CO_2 $\delta^{13}C$ signature from the burning of fossil fuels (Keeling 1979). This was not observed in the deforested soil because of sediment mixing in the upper layers. The 10-fold larger soil mixing at deforested sites could have been caused by trampling by harvesters and dragging of logs during clearcutting. As shown in the felling of terrestrial forests, most soil damage occurs during wood transportation from the stump area to the landings (Jamshidi and others 2008; Cambi and others 2015). In addition, 10 years of subsequent exposure of reworked soils could have led to increased erosion of cleared soils with tides and run off as observed in Grellier and others (2017) two years after mangrove clearing. However, unlike the study of Grellier et al. (2018) in Vietnam, our data do not show a winnowing of fine particles at deforested sites. Indeed, our deforested soils contained twice as much clay per soil volume as intact soils throughout the soil profile suggesting that their location at the bottom of the U-shaped bay might favor the retention of sediments regardless of mangrove loss. This is confirmed by similar average $^{210}Pb_{xs}$ inventories measured within deforested and low-DBD intact soils. Despite the large variability at intact sites, results suggest that net soil erosion was not enhanced at deforested sites, hence could not explain the depletion of C and N observed in the upper 14 g cm^{-2}.

In our study, the observed C depletion measured in the upper 14 g cm^{-2} of deforested soils could have occurred largely because of the lack of new litter supply and the enhanced C remineralization promoted by soil physical mixing and the exposure of deforested surface soils to direct solar radiation after canopy loss (Bosire and others 2003; Lovelock and others 2017a). Soil mixing can impact C processing in multiple ways: by aeration, by mixing labile organic matter to deeper layers as well as by breaking the soil structure and exposing organic material previously

446 protected by burial (Burdige 2007; Middelburg 2018). All these processes promote C mineralization
447 and CO_2 emissions to the atmosphere (Lovelock and others 2017a). Assuming that low-DBD intact
448 soils best represent deforested soils before mangrove clearance, we estimated that soil C loss caused
449 by deforestation accounted for 50 ± 14 Mg C ha^{-1}, as indicated by the comparison of C stocks over
450 the upper 14 g cm^{-2} (Table 4). This C loss would have occurred at a mean rate of 5.0 ± 1.4 Mg C ha^{-1}
451 yr^{-1} during the 10-yr following clearcutting, which is 4.5 times higher than the annual C
452 sequestration rate estimated in low-DBD intact soils.

453 Roughly 20% of the upper 1-m C stock, and 45% of that accumulated in the last century,
454 would have been lost since deforestation relative to low-DBD intact soils. The magnitude of C loss
455 in the upper 14 g cm^{-2} was, however, as important as the variability of the C stocks in the upper 45 g
456 cm^{-2} (apparent ~1 m) of low-DBD and deforested soils. This may explain why differences in soil C
457 stocks at a depth of 1 meter could not be detected in this study and others (Lang'at and others 2014),
458 unless specific soil mass-depth increments that encompass similar accumulation periods were
459 analyzed. Proportional changes in N stocks were comparable. Results indicated a preferential loss of
460 N with age (or depth) under natural conditions that was enhanced with disturbance as deforested
461 soils showed a greater increase in average C:N ratios than intact soils throughout the upper 14 cm^{-2}
462 (Fig. S2). Soil C loss occurred in addition to the loss from standing biomass, which was estimated at
463 130 ± 14 Mg C ha^{-1} (Fig. 6). Soil C and N losses (versus tree biomass) could have been lower if
464 deforestation had occurred for mangroves in high-DBD intact plots given their smaller organic C and
465 N soil content (Lovelock and others 2017a).
466
467 Pathways for soil C loss likely include atmospheric emissions as CO_2 and lateral export as
468 dissolved C to coastal waters. Most research has focused on constraining C losses from soils as
469 fluxes of CO_2 following disturbance (e.g., references in Table 5). For comparison, the mean C loss
470 rate estimated in deforested soils here is equivalent to emissions of 18 ± 5 Mg CO_2 ha^{-1} y^{-1}, which

compare well with CO_2 efflux measurements after mangrove clearing reported by others (e.g., Lang'at and others 2014; Bulmer and others 2015; Grellier and others 2017) and is similar to CO_2 emissions inferred from peat collapse due to hurricane damage (Cahoon and others 2003) and from stock change methods after conversion to cattle pastures (Kauffman and others 2016) (Table 5). However, our estimated emissions were about 4 times lower than those reported when soils were excavated and converted to shrimp ponds (Sidik and Lovelock 2013; Kauffman and others 2014, 2018).

Lateral fluxes of dissolved C from cleared mangroves have been rarely considered (Sippo and others 2019), despite this being the major fate of C from healthy mangrove forests (Bouillon and others 2008; Maher and others 2018). Although our data were limited, DOC concentrations of waters nearshore of the deforested and intact forests were very high, even during flood tide, far exceeding those typical of seawater and coastal waters (~100 and 200 μmol C L^{-1}, respectively; Barrón and Duarte 2015), which confirms the importance of mangrove forests, whether intact or degraded, as a source of DOC to the coastal ocean. The lack of samples taken along river sources and coastal areas at the same tidal stage precluded assessing the effect of mangrove deforestation on the magnitude of DOC export. However, because mangrove deforestation limits the supply of new C inputs to the forest floor, the presence of high DOC concentrations (median: 2,000 μmol C L^{-1}) in waters nearshore of the cleared area even 10 years after deforestation may suggest that existing soil C reserves are being depleted. This is consistent with the findings by Maher and others (2017), who showed that even aged sequestered C in mangroves is susceptible to remineralization and export to the coastal ocean. This process reintroduces aged C into the modern C cycle and thus could lead to increased CO_2 emissions in coastal waters if bioavailable and oxidized (Drake and others 2019).

Mangrove deforestation promotes changes in soil physico-chemical properties and functions (soil C storage, nutrient processing and vertical accretion) (Grellier and others 2017; Otero and

others 2017) that enhance the susceptibility of C stocks to remineralization, resulting in potential changes in C fluxes to the coast and large amounts of CO_2 to the atmosphere. Using "*tier 2*" approaches, we estimate that mangrove deforestation for timber and charcoal in Tsimipaika Bay has resulted in measurable reductions in total ecosystem C stocks that represents a combined potential loss of 180 ± 20 Mg C ha^{-1} from standing biomass and soil organic C stocks in the 10 years since clearing. While C losses from standing biomass are unequivocal and could contribute significantly to CO_2 emissions if harvested timber is used as fuel-wood, emissions from soils are more difficult to assess because of the large soil heterogeneity of intact mangrove forests and the partial export of C to adjacent aquatic coastal systems. However, our data show that even in the absence of excavation of soils (e.g. for aquaculture ponds, Kauffman and others 2014) or soil erosion, C losses would have occurred at a rate that is 4.5 times that which C accumulates in soils of intact closed-canopy forests. In Tsimipaika-Ambaro Bay, closed-canopy mangrove forests cover 14,000 ha in contrast to 1,000 ha of deforested soils, which thereby reduce the annual C sequestration capacity of the dense mangrove ecosystem by 32%. Nation-wide, Madagascar has lost 20,300 ha of mangroves between 2000 and 2010 (Jones and others 2016a). If our results are broadly representative, C loss from cleared mangrove soils could be significant and account for approximately 20% of total national C emissions from fossil fuel combustion over that 10 year period (Boden and others 2017). Although rates of mangrove deforestation have slowed in the last decade (Hamilton and Casey 2016), deforestation of mangroves is still a nationally important source of emissions for many nations, particularly those with high rates of deforestation and moderate emissions from other sectors (Taillardat and others 2018). Our results show the importance of avoiding CO_2 emissions associated with mangrove deforestation, particularly, given that establishing high rates of carbon uptake through restoration of mangroves can take decades (Osland and others 2012). Thus, conservation is an effective mechanism for reducing CO_2 emissions. Conservation projects seeking to account for C emissions and removals

should take into consideration avoided emissions from soils as well as from loss of biomass, even in cases where excavation of soils has not taken place.

Data availability

Data supporting the findings of this study (DBD, water content, grains size distribution, C and N contents, $\delta^{13}C$ and $\delta^{15}N$, ^{210}Pb and DOC) are available at https://ddd.uab.cat/record/216456 with the identifier doi:10.5565/ddd.uab.cat/216456

Acknowledgements

We thank the Blue Ventures team in Madagascar and Samantha Ridgway and Gloria Salgado from Edith Cowan University for their help in the field and lab work. Funding was provided to PM and JGO by the Generalitat de Catalunya (Grant 2017 SGR-1588) and to PM through an Australian Research Council LIEF Project (LE170100219). Funding was provided to MH and CBN through a South African NRF Research Development grant (Grant No: 105724). Blue Ventures was funded by the GEF Blue Forests Project. This work is contributing to the ICTA 'Unit of Excellence' (MinECo, MDM2015-0552). AA-O was supported by "Obra Social la Caixa" (LCF/BQ/ES14/10320004) and by the NOAA C&GC Postdoctoral Fellowship Program administered by UCAR-CPAESS under award #NA18NWS4620043B.

References

Adame MF, Zakaria RM, Fry B, Chong VC, Then YHA, Brown CJ, Lee SY. 2018. Loss and recovery of carbon and nitrogen after mangrove clearing. Ocean Coast Manag 161:117–26.

Alongi DM. 2002. Present state and future of the world's mangrove forests. Environ Conserv 29:331–49.

Appleby PG. 2001. Chronostratigraphic Techniques in Recent Sediments. In: Tracking Environmental Change Using Lake Sediments. Vol. 1. Springer Netherlands. pp 171–203.

Arata L, Meusburger K, Frenkel E, A'Campo-Neuen A, Iurian AR, Ketterer ME, Mabit L, Alewell C. 2016. Modelling Deposition and Erosion rates with RadioNuclides (MODERN) - Part 1: A new conversion model to derive soil redistribution rates from inventories of fallout radionuclides. J Environ Radioact 162–163:45–55.

Arias-Ortiz A, Masqué P, Garcia-Orellana J, Serrano O, Mazarrasa I, Marbà N, Lovelock CE, Lavery P, Duarte CM. 2018. Reviews and syntheses: 210Pb-derived sediment and carbon accumulation rates in vegetated coastal ecosystems: setting the record straight. Biogeosciences 15:6791–818.

Atwood TB, Connolly RM, Almahasheer H, Carnell PE, Duarte CM, Ewers Lewis CJ, Irigoien X, Kelleway JJ, Lavery PS, Macreadie PI, Serrano O, Sanders CJ, Santos I, Steven ADL, Lovelock CE. 2017. Global patterns in mangrove soil carbon stocks and losses. Nat Clim Chang 7:523–8.

Balesdent J, Chenu C, Balabane M. 2000. Relationship of soil organic matter dynamics to physical protection and tillage. Soil Tillage Res 53:215–30.

Barbier EB, Hacker SD, Kennedy C, Koch EW, Stier AC, Silliman BR. 2011. The value of estuarine and coastal ecosystem services. Ecol Monogr 81:169–93.

Barrón C, Duarte CM. 2015. Global Biogeochemical Cycles from the coastal ocean. Global Biogeochem Cycles 29:1725–38.

Benner R, Strom M. 1993. A critical evaluation of the analytical blank associated with. MarChem 41:153–60.

Benson L, Glass L, Jones TG, Ravaoarinorotsihoarana L, Rakotomahazo C. 2017. Mangrove carbon stocks and ecosystem cover dynamics in southwest Madagascar and the implications for local management. Forests 8:1–21.

Bianchi TS. 2011. The role of terrestrially derived organic carbon in the coastal ocean: A changing paradigm and the priming effect. Proc Natl Acad Sci 108:19473–81.

567 Boden TA, Marland G, Andres RJ. 2017. Global, Regional, and National Fossil-Fuel CO2 Emissions.
568 https://cdiac.ess-dive.lbl.gov/trends/emis/overview_2014.html. Last accessed 13/10/2019

569 Bosire JO, Dahdouh-Guebas F, Kairo JG, Koedam N. 2003. Colonization of non-planted mangrove species
570 into restored mangrove stands in Gazi Bay, Kenya. Aquat Bot 76:267–79.

571 Boto K, Wellington J. 1984. Soil characteristics and nutrient status in a northern Australian mangrove forest.
572 Estuaries.

573 Bouillon S, Borges A V., Castañeda-Moya E, Diele K, Dittmar T, Duke NC, Kristensen E, Lee SY, Marchand
574 C, Middelburg JJ, Rivera-Monroy VH, Smith TJ, Twilley RR. 2008. Mangrove production and carbon
575 sinks: A revision of global budget estimates. Global Biogeochem Cycles 22:1–12.

576 Breithaupt JL, Smoak JM, Smith TJ, Sanders CJ, Hoare A. 2012. Organic carbon burial rates in mangrove
577 sediments: Strengthening the global budget. Global Biogeochem Cycles 26.

578 Bulmer RH, Lundquist CJ, Schwendenmann L. 2015. Sediment properties and CO2 efflux from intact and
579 cleared temperate mangrove forests. Biogeosciences 12:6169–80.

580 Burdige DJ. 2007. Preservation of organic matter in marine sediments: Controls, mechanisms, and an
581 imbalance in sediment organic carbon budgets? Chem Rev 107:467–85.

582 Cahoon DR, Hensel P, Rybczyk J, McKee KL, Proffitt CE, Perez BC. 2003. Mass tree mortality leads to
583 mangrove peat collapse at Bay Islands, Honduras after Hurricane Mitch. J Ecol 91:1093–105.

584 Cambi M, Certini G, Neri F, Marchi E. 2015. The impact of heavy traffic on forest soils: A review. For Ecol
585 Manage 338:124–38.

586 Chave J, Andalo C, Brown S, Cairns MA, Chambers JQ, Eamus D, Fölster H, Fromard F, Higuchi N, Kira T,
587 Lescure J-P, Nelson BW, Ogawa H, Puig H, Riéra B, Yamakura T. 2005. Tree allometry and improved
588 estimation of carbon stocks and balance in tropical forests. Oecologia 145:87–99.

589 Chave J, Coomes D, Jansen S, Lewis SL, Swenson NG, Zanne AE. 2009. Towards a worldwide wood
590 economics spectrum. Ecol Lett 12:351–66.

591 Chmura GL, Anisfeld SC, Cahoon DR, Lynch JC. 2003. Global carbon sequestration in tidal, saline wetland
592 soils. Global Biogeochem Cycles 17:1111.

593 Clough BF, Scott K. 1989. Allometric relationships for estimating above-ground biomass in six mangrove
594 species. For Ecol Manage 27:117–27.

595 Cole TG, Ewel KC, Devoe NN. 1999. Structure of mangrove trees and forests in Micronesia. For Ecol
596 Manage 117:95–109.

597 Delgado M, de Jonge VN, Peletier H. 1991. Experiments on resuspension of natural microphytobenthos
598 populations. Mar Biol 108:321–8.

599 Diochon A, Kellman L, Beltrami H. 2009. Looking deeper: An investigation of soil carbon losses following
600 harvesting from a managed northeastern red spruce (Picea rubens Sarg.) forest chronosequence. For Ecol
601 Manage 257:413–20.

602 Donato DC, Kauffman JB, Murdiyarso D, Kurnianto S, Stidham M. 2011. Mangroves among the most
603 carbon-rich forests in the tropics. Nat Geosci 4:1–5.

604 Drake TW, Van Oost K, Barthel M, Bauters M, Hoyt AM, Podgorski DC, Six J, Boeckx P, Trumbore SE,
605 Cizungu Ntaboba L, Spencer RGM. 2019. Mobilization of aged and biolabile soil carbon by tropical
606 deforestation. Nat Geosci 12:541–6.

607 Duke N, Wolanski E. 2001. Muddy Coastal Waters and Depleted Mangrove Coastlines — Depleted Seagrass
608 and Coral Reefs. In: Wolanski E, editor. Oceanographic Processes of Coral Reefs. Physical and Biology
609 Links in the Great Barrier Reef. Washington, DC: CRC Press. pp 77–91.

610 Ellison AM, Farnsworth EJ. 1996. Anthropogenic Disturbance of Caribbean Mangrove Ecosystems: Past
611 Impacts, Present Trends, and Future Predictions. Biotropica 28:549.

612 FAO [Food and Agriculture Organization of the United Nations]. 2007. The world's mangroves 1980-2005.
613 Rome, Italy

614 Ferreira TO, Otero XL, de Souza Junior VS, Vidal-Torrado P, Macías F, Firme LP. 2010. Spatial patterns of

soil attributes and components in a mangrove system in Southeast Brazil (São Paulo). J Soils Sediments 10:995–1006.

Fourqurean JW, Schrlau JE. 2003. Changes in nutrient content and stable isotope ratios of C and N during decomposition of seagrasses and mangrove leaves along a nutrient availability gradient in Florida Bay, USA. Chem Ecol 19:373–90.

Gifford RM, Roderick ML. 2003. Soil carbon stocks and bulk density: Spatial or cumulative mass coordinates as a basis of expression? Glob Chang Biol 9:1507–14.

Gillis LG, Belshe EF, Narayan GR. 2017. Deforested Mangroves Affect the Potential for Carbon Linkages between Connected Ecosystems. Estuaries and Coasts 40:1207–13.

Glew JR, Smol JP, Last WM. 2001. Sediment Core Collection and Extrusion. In: Last WM, Smol JP, editors. Tracking Environmental Change Using Lake Sediments: Basin Analysis, Coring, and Chronological Techniques. Dordrecht: Springer Netherlands, Dordrecht. pp 73–105.

Granek E, Ruttenberg BI. 2008. Changes in biotic and abiotic processes following mangrove clearing. Estuar Coast Shelf Sci 80:555–62.

Grellier S, Janeau JL, Dang Hoai N, Nguyen Thi Kim C, Le Thi Phuong Q, Pham Thi Thu T, Tran-Thi NT, Marchand C. 2017. Changes in soil characteristics and C dynamics after mangrove clearing (Vietnam). Sci Total Environ 593–594:654–63.

Haines WB. 1923. The volume-changes associated with variations of water content in soil. J Agric Sci 13:296–310.

Hamilton SE, Casey D. 2016. Creation of a high spatio-temporal resolution global database of continuous mangrove forest cover for the 21st century (CGMFC-21). Glob Ecol Biogeogr 25:729–38.

Hargis TG, Twilley RR. 1994. Improved coring device for measuring soil bulk density in a Louisiana deltaic marsh. J Sediment Res 64:681–3.

Herr D, von Unger M, Laffoley D, McGivern A. 2017. Pathways for implementation of blue carbon

initiatives. Aquat Conserv Mar Freshw Ecosyst 27:116–29.

IPCC. 2014. 2013 Supplement to the 2006 IPCC Guidelines for National Greenhouse Gas Inventories: Wetlands Task Force on National Greenhouse Gas Inventories: Wetlands. (Hiraishi T, Krug T, Kiyoto T, Srivastava N, Jamsranjav B, Fukuda M, Troxler T, editors.). Switzerland: IPCC

Jamshidi R, Jaeger D, Raafatnia N, Tabari M. 2008. Influence of Two Ground-Based Skidding Systems on Soil Compaction Under Different Slope and Gradient Conditions. Int J For Eng 19:9–16.

Jones TG, Glass L, Gandhi S, Ravaoarinorotsihoarana L, Carro A, Benson L, Ratsimba HR, Giri C, Randriamanatena D, Cripps G. 2016a. Madagascar's mangroves: Quantifying nation-wide and ecosystem specific dynamics, and detailed contemporary mapping of distinct ecosystems. Remote Sens 8.

Jones TG, Ratsimba HR, Carro A, Ravaoarinorotsihoarana L, Glass L, Teoh M, Benson L, Cripps G, Giri C, Zafindrasilivonona B, Raherindray R, Andriamahenina Z, Andriamahefazafy M. 2016b. The Mangroves of Ambanja and Ambaro Bays, Northwest Madagascar: Historical Dynamics, Current Status and Deforestation Mitigation Strategy Trevor. In: Diop S et al., editor. Estuaries: A Lifeline of Ecosystem Services in the Western Indian Ocean. Springer International Publishing Switzerland. pp 67–85.

Jones TG, Ratsimba HR, Ravaoarinorotsihoarana L, Cripps G, Bey A. 2014. Ecological Variability and Carbon Stock Estimates of Mangrove Ecosystems in Northwestern Madagascar. Forests 5:177–205.

Kauffman JB, Bernardino AF, Ferreira TO, Bolton NW, Eduardo L, Gabriel DOG, Nobrega N. 2018. Shrimp ponds lead to massive loss of soil carbon and greenhouse gas emissions in northeastern Brazilian mangroves. Ecol Evol 8:5530–40.

Kauffman JB, Donato DC. 2012. Protocols for the measurement, monitoring and reporting of structure, biomass and carbon stocks in mangrove forests. Bogor, Indonesia: CIFOR

Kauffman JB, Heider C, Norfolk J, Payton F. 2014. Carbon stocks of intact mangroves and carbon emissions arising from their conversion in the Dominican Republic. Ecol Appl 24:518–27.

Kauffman JB, Hernandez Trejo H, del Carmen Jesus Garcia M, Heider C, Contreras WM. 2016. Carbon

664 stocks of mangroves and losses arising from their conversion to cattle pastures in the Pantanos de Centla,
665 Mexico. Wetl Ecol Manag 24:203–16.

666 Kauffman JB, Thorpe AS, Brookshire ENJ. 2004. Livestock exclusion and belowground ecosystem responses
667 in riparian meadows of Eastern Oregon. Ecol Appl 14:1671–9.

668 Keeling CD. 1979. The Suess effect: 13Carbon-14Carbon interrelations. Environ Int 2:229–300.

669 Kennedy P, Kennedy H, Papadimitriou S. 2005. The effect of acidification on the determination of organic
670 carbon, total nitrogen and their stable isotopic composition in algae and marine sediment. Rapid
671 Commun Mass Spectrom 19:1063–8.

672 Komiyama A, Poungparn S, Kato S. 2005. Common allometric equations for estimating the tree weight of
673 mangroves. J Trop Ecol 21:471–7.

674 Krauss KW, Cahoon DR, Allen JA, Ewel KC, Lynch JC, Cormier N. 2010. Surface Elevation Change and
675 Susceptibility of Different Mangrove Zones to Sea-Level Rise on Pacific High Islands of Micronesia.
676 Ecosystems 13:129–43.

677 Krishnaswamy S, Lal D, Martin JM, Meybeck M. 1971. Geochronology of lake sediments. Earth Planet Sci
678 Lett 11:407–14.

679 Kristensen E, Alongi DM. 2006. Control by fiddler crabs (*Uca vocans*) and plant roots (*Avicennia marina*)
680 on carbon, iron, and sulfur biogeochemistry in mangrove sediment. Limnol Oceanogr 51:1557–71.

681 Labrière N, Locatelli B, Laumonier Y, Freycon V, Bernoux M. 2015. Soil erosion in the humid tropics: A
682 systematic quantitative review. Agric Ecosyst Environ 203:127–39.

683 Lang'at JKS, Kairo JG, Mencuccini M, Bouillon S, Skov MW, Waldron S, Huxham M. 2014. Rapid losses of
684 surface elevation following tree girdling and cutting in tropical mangroves. PLoS One 9:1–8.

685 Lovelock CE, Atwood T, Baldock J, Duarte CM, Hickey S, Lavery PS. 2017a. Assessing the risk of carbon
686 dioxide emissions from blue carbon ecosystems. Front Ecol Environ 15:257–65.

687 Lovelock CE, Fourqurean JW, Morris JT. 2017b. Modeled CO2 Emissions from Coastal Wetland Transitions

688 to Other Land Uses: Tidal Marshes, Mangrove Forests, and Seagrass Beds. Front Mar Sci 4:1–11.

689 Lovelock CE, Ruess R, Feller I. 2011. CO2 efflux from cleared mangrove peat. PLoS One 6:e21279.

690 Lundquist CJ, Morrisey DJ, Gladstone-Gallagher R V., Swales A. 2014. Managing Mangrove Habitat
691 Expansion in New Zealand. In: Mangrove Ecosystems of Asia. New York, NY: Springer New York. pp
692 415–38.

693 Macnae W. 1969. A General Account of the Fauna and Flora of Mangrove Swamps and Forests in the Indo-
694 West-Pacific Region. Adv Mar Biol 6:73–270.

695 Maher DT, Call M, Santos IR, Sanders CJ. 2018. Beyond burial: Lateral exchange is a significant atmospheric
696 carbon sink in mangrove forests. Biol Lett 14.

697 Maher DT, Santos IR, Schulz KG, Call M, Jacobsen GE, Sanders CJ. 2017. Blue carbon oxidation revealed by
698 radiogenic and stable isotopes in a mangrove system. Geophys Res Lett 44:4889–96.

699 McKee KL. 2011. Biophysical controls on accretion and elevation change in Caribbean mangrove
700 ecosystems. Estuar Coast Shelf Sci 91:475–83.

701 McLeod E, Chmura GL, Bouillon S, Salm R, Björk M, Duarte CM, Lovelock CE, Schlesinger WH, Silliman
702 BR. 2011. A blueprint for blue carbon: Toward an improved understanding of the role of vegetated
703 coastal habitats in sequestering CO2. Front Ecol Environ 9:552–60.

704 Middelburg JJ. 2018. Reviews and syntheses: To the bottom of carbon processing at the seafloor.
705 Biogeosciences 15:413–27.

706 Morton RA, White WA. 1997. Characteristics of and corrections for core shortening in unconsolidated
707 sediments. J Coast Res 13:761–9.

708 Ong JE. 1993. Mangroves - a carbon source and sink. Chemosphere 27:1097–107.

709 Osland MJ, Spivak AC, Nestlerode JA, Lessmann JM, Almario AE, Heitmuller PT, Russell MJ, Krauss KW,
710 Alvarez F, Dantin DD, Harvey JE, From AS, Cormier N, Stagg CL. 2012. Ecosystem Development
711 After Mangrove Wetland Creation: Plant-Soil Change Across a 20-Year Chronosequence. Ecosystems

712 15:848–66.

713 Otero XL, Méndez A, Nóbrega GN, Ferreira TO, Meléndez W, Macías F. 2017. High heterogeneity in soil
714 composition and quality in different mangrove forests of Venezuela. Environ Monit Assess 189.

715 Rasolofo M, Ramilijaona O. 2009. Variability in the abundance and recruitment of Fenneropenaeus indicus
716 and Metapenaeus monoceros postlarvae and juveniles in Ambaro Bay mangroves of Madagascar. Nat
717 Faune 24:103–9.

718 Sanchez-Cabeza JA, Masqué P, Ani-Ragolta I. 1998. 210Pb and210Po analysis in sediments and soils by
719 microwave acid digestion. J Radioanal Nucl Chem 227:19–22.

720 Semeniuk V. 1996. Coastal forms and Quaternary processes along the arid Pilbara coast of northwestern
721 Australia. Palaeogeogr Palaeoclimatol Palaeoecol 123:49–84.

722 Sidik F, Lovelock CE. 2013. CO2 Efflux from Shrimp Ponds in Indonesia. PLoS One 8:6–9.

723 Sippo JZ, Maher DT, Schulz KG, Sanders CJ, McMahon A, Tucker J, Santos IR. 2019. Carbon outwelling
724 across the shelf following a massive mangrove dieback in Australia: Insights from radium isotopes.
725 Geochim Cosmochim Acta 253:142–58.

726 Stover HJ, Henry HAL. 2018. Soil homogenization and microedges: perspectives on soil-based drivers of
727 plant diversity and ecosystem processes. Ecosphere 9:e02289.

728 Taillardat P, Friess DA, Lupascu M. 2018. Mangrove blue carbon strategies for climate change mitigation are
729 most effective at the national scale. Biol Lett 14:20180251.

730 Thampanya U, Vermaat JE, Sinsakul S, Panapitukkul N. 2006. Coastal erosion and mangrove progradation of
731 Southern Thailand. Estuar Coast Shelf Sci 68:75–85.

732 Twilley RR, Day JW. 2012. Mangrove Wetlands. In: W. Day J, C. Crump B, Kemp WM, Yáñez-Arancibia A,
733 editors. Estuarine Ecology. Second. Hoboken, NJ, USA: John Wiley & Sons, Inc. pp 165–202.

734 Wendt JW, Hauser S. 2013. An equivalent soil mass procedure for monitoring soil organic carbon in multiple
735 soil layers. Eur J Soil Sci 64:58–65.

Wentworth C. 1922. A scale of grade and class terms for clastic sediments. J Geol 30:377–92.

Yanai RD, Currie WS, Goodale CL. 2003. Soil carbon dynamics after forest harvest: An ecosystem paradigm reconsidered. Ecosystems 6:197–212.

Zanne AE, Lopez-Gonzalez G, Coomes DA, Ilic J, Jansen S, Lewis SL, Miller RB, Swenson NG, Wiemann MC, Chave J. 2009. Data from: towards a worldwide wood economics spectrum. Dryad Digit Repos.

Zummo LM, Friedland AJ. 2011. Soil carbon release along a gradient of physical disturbance in a harvested northern hardwood forest. For Ecol Manage 261:1016–26.

744 **Table Legends**

745 **Table 1. Site characteristics for sampled mangrove plots of Tsimipaika Bay, Madagascar.**
746 Average values for tree height (m), diameter at breast height (dbh) (cm) and trees per hectare (ha^{-1}).
747 Dead tree density in deforested plots equals stump density and regeneration density equals number of
748 seedlings per unit area. Cc stands for Closed-canopy, De for Deforested, and n.d. for "no data".
749

750 **Table 2. Intact and deforested soil characteristics over the upper 45 g·cm^{-2}.** U and t values of
751 Mann-Witney and Two-sample t- test results are included for the comparison of soil properties
752 between intact and deforested mangrove soils. ***Significant at 0.001 level, ** at 0.01 and * at 0.05.
753 NS is not significant.
754

755 **Table 3. Sedimentation rates and $^{210}Pb_{xs}$ inventories in intact and deforested soils**. The
756 uncertainties represent the SE resulting from the CF:CS model to obtain the mass accumulation and
757 accretion rates (MAR and SAR), and ^{226}Ra specific activities represent the mean and the standard
758 deviation (n = 5 at each core). Accretion rates (SAR) were corrected for core shortening thus should
759 be considered as apparent rates.
760

761 **Table 4. Soil carbon and nitrogen accumulation rates and stocks.** Stocks in the upper 1 meter are
762 also included for reporting purposes and should be considered apparent stocks due to the soil
763 shortening correction applied.
764

765 **Table 5. Published C loss rates from degraded mangrove soils.** To facilitate comparison among
766 most other assessments and this study, C losses are expressed as CO_2 equivalents (CO_2e) obtained by
767 multiplying C loss rate by 3.67. Where rates of C loss were not reported, we estimated a mean annual
768 C loss as the total soil C stock loss divided by the time since disturbance.

769 **Table 1.**

Core ID	Species dominance	Geomorphic position	Tidal inundation	Tree height (m)	dbh (cm)	Live Tree Density (ha^{-1})	Dead Tree Density (ha^{-1})	Regeneration density (ha^{-1})	Canopy cover (%)	Total biomass C (Mg C ha^{-1})
Cc18	*S. alba*	Riverine	freq.	8	18	800	0	0	94	160
Cc19	*B. gymnorhiza*	Riverine	infreq.	10	13	2400	200	5200	95	254
Cc20	*R. mucronata*	Basin	freq.	9	10	4700	200	800	95	238
Cc28	*R. mucronata*	Basin	infreq.	n.d.	10	2900	400	2800	93	128
Cc29	*R. mucronata*	Riverine	freq.	9	9	2900	600	0	98	113
De27	*B. gymnorhiza*	Riverine	freq.	5	7	200	100	0	0.9	3.0
De30	*B. gymnorhiza*	Basin	infreq.			0	1000	2000	0.2	1.8
De31	*R. mucronata*	Basin	freq.			0	100	0	0.2	0.1
De32	*C. tagal*	Riverine	infreq.			0	3000	2400	7	1.4
De33	*C. tagal*	Basin	infreq.			0	11400	4400	0.2	9.5

770

771 **Table 2.**

Soil Class	**Core ID**	**Statistic**	**Water content (%)**	**DBD (g cm^{-3})**	**C (%DW)**	**N (%DW)**	**C:N**	**Clay (%)**
High-DBD Intact	Cc19, 20	Mean ± SE	30.1 ± 0.6	0.881 ± 0.013	2.40 ± 0.08	0.095 ± 0.003	28.6 ± 0.6	11.2 ± 1.0
		Median	29.1	0.88	2.3	0.093	28.0	10.3
Low-DBD Intact	Cc18, 28, 29	Mean ± SE	56.9 ± 0.7	0.347 ± 0.008	7.7 ± 0.2	0.314 ± 0.012	29.6 ± 0.4	15.3 ± 1.1
		Median	58.7	0.36	7.4	0.30	28.9	15
Intact (all)	Cc18, 19, 20, 28, 29	Mean ± SE	47.4 ± 0.9	0.580 ± 0.015	5.7 ± 0.2	0.231 ± 0.011	29.3 ± 0.3	14.0 ± 0.8
		Median	48.7	0.49	5.5	0.20	28.8	13.1
Deforested	De27, 30, 31, 32, 33	Mean ± SE	44.5 ± 0.4	0.415 ± 0.006	5.11 ± 0.15	0.173 ± 0.003	33.5 ± 0.6	28.1 ± 1.3
		Median	44.3	0.41	4.8	0.17	32.6	26.4
Treatment					Prob>|U|			Prob>|t|
Intact (all) vs. Deforested			0.007 **	$1.1 \cdot 10^{-9}$ ***	1.00 NS	0.11 NS	$2.6 \cdot 10^{-8}$***	$1.1 \cdot 10^{-14}$ ***
High-DBD Intact vs. Deforested			0 ***	$5.6 \cdot 10^{-53}$***	$4.1 \cdot 10^{-26}$***	$1.7 \cdot 10^{-25}$***	$7.0 \cdot 10^{-6}$***	$9.4 \cdot 10^{-10}$ ***
Low-DBD Intact vs. Deforested			0 ***	$2.6 \cdot 10^{-9}$***	0***	0***	$2.6 \cdot 10^{-6}$***	$3.4 \cdot 10^{-10}$ ***

772

773

774

775 **Table 3.**

Core ID	Type	Mixing depth	$^{210}Pb_{xs}$ horizon	^{226}Ra	MAR	SAR	$^{210}Pb_{xs}$ inventory
		g cm^{-2}	g cm^{-2}	Bq kg^{-1}	g cm^{-2} yr^{-1}	mm yr^{-1}	Bq m^{-2}
Cc19	High-DBD	1.7	7	13.2 ± 1.5	0.070 ± 0.014	0.85 ± 0.11	500 ± 50
Cc20		2.0	9	12.6 ± 1.3	0.099 ± 0.013	1.11 ± 0.15	690 ± 40
Cc18	Low-DBD	0.8	11	19 ± 4	0.094 ± 0.007	4.1 ± 0.2	3170 ± 90
Cc28		1.2	13	13 ± 4	0.10 ± 0.02	2.3 ± 0.4	1920 ± 80
Cc29		1.5	17	13 ± 2	0.223 ± 0.012	8.4 ± 0.4	4750 ± 80
Mean (SE) high-DBD		**1.9 ± 0.2**	**8.0 ± 0.8**		**0.085 ± 0.015**	**0.98 ± 0.13**	**600 ± 100**
Mean (SE) low-DBD		**1.2 ± 0.2**	**13 ± 2**		**0.14 ± 0.04**	**5 ± 2**	**3280 ± 820**
Mean (SE) Intact		**1.4 ± 0.2**	**11 ± 2**		**0.12 ± 0.03**	**3.4 ± 1.4**	**2210 ± 800**
De27	Deforested	4	14	25 ± 6			1940 ± 90
De30		6	14	18 ± 4			1200 ± 70
De31		25	24	13.0 ± 1.4			2580 ± 90
De32		8	10	21 ± 6			1870 ± 170
De33		26	26	15 ± 2			2040 ± 100
Mean (SE) Deforested		**14 ± 5**	**18 ± 3**				**1930 ± 220**

776

777 **Table 4.**

Core ID	Type	C accumulation rate	N accumulation rate	C stock		N stock		C stock	N stock
				0-14 g cm^{-2}	0-45 g cm^{-2}	0-14 g cm^{-2}	0-45 g cm^{-2}	1 m	1 m
		g C m^{-2} yr^{-1}	g N m^{-2} yr^{-1}	Mg C ha^{-1}		Mg N ha^{-1}		Mg C ha^{-1}	Mg N ha^{-1}
Cc19	High-DBD	18 ± 4	0.68 ± 0.14	32	109	1.3	4.1	218	8
Cc20		25 ± 3	1.18 ± 0.15	33	91	1.5	3.9	192	8
Cc18	Low-DBD	75 ± 6	3.4 ± 0.3	108	279	4.4	11	190	7
Cc28		64 ± 11	2.2 ± 0.4	87	248	3.1	8.9	250	9
Cc29		176 ± 9	7.3 ± 0.4	135	305	5.8	13	229	9
Mean (SE) High-DBD Intact		**21 ± 3**	**0.9 ± 0.3**	**32.4 ± 0.4**	**100 ± 9**	**1.40 ± 0.12**	**3.99 ± 0.06**		
Mean (SE) Low-DBD Intact		**110 ± 40**	**4 ± 2**	**110 ± 14**	**280 ± 20**	**4.4 ± 0.8**	**11.0 ± 1.1**		
Mean (SE) Intact		**70 ± 30**	**3.0 ± 1.2**	**80 ± 20**	**200 ± 40**	**2.9 ± 0.8**	**8 ± 2**	**220 ± 10**	**8.3 ± 0.3**
De27	Deforested			64	268	2.1	8	268	8
De30				69	344	2.2	10	279	8
De31				53	194	2.1	7	181	6
De32				57	261	3.1	10	166	6
De33				52	170	2.2	7	135	5
Mean (SE) deforested				**60 ± 3**	**250 ± 30**	**2.3 ± 0.2**	**8.2 ± 0.7**	**210 ± 30**	**7.0 ± 0.5**

778

779 **Table 5.**

References	Disturbance type	Years since disturbance	Method for estimating C loss	CO_2 emissions Mg CO_2e ha^{-1} yr^{-1}		
This study	**Clearing**	**10**	**C stock change**	**18**	**±**	**5**
Grellier and others (2017)	Clearing	2	C stock change	37		
			Gas flux chambers	4	±	7
Bulmer and others (2015)	Clearing	0.1-8	Gas flux chambers	21	±	6
Lang'at and others (2014)	Clearing	2	C stock change	35	±	45
			Gas flux chambers	25	±	7
Lovelock and others (2011)	Clearing	1	Gas flux chambers	106		
		20		30		
Kauffman and others (2016b)	Conversion to cattle pastures	7	C stock change	16	±	6
		30		7	±	2
Kauffman and others (2014)	Conversion to aquaculture	29	C stock change	82		
Kauffman and others (2018)	Conversion to aquaculture	10-12	C stock change	107	±	40
		10-12		184	±	10
		8		13	±	5
Sidik and Lovelock (2013)	Conversion to aquaculture	25	Gas flux chambers in pond floor	16		
			Gas flux chambers in pond walls	44		
Cahoon and others (2003)	Hurricane damage	2	Change in soil volume	19		

780

781

782 **Figure Legends**

783 **Figure 1.** Map of Tsimipaika Bay in northwest Madagascar with sampled plot locations in
784 intact and deforested mangrove areas. St. labels are surface water sampling locations.

785

786 **Figure 2.** Principal component analysis on physico-chemical properties of soils from
787 deforested and intact mangroves. Biplot of variable vectors showing correlation between the
788 variables, the component and individual factor map. Superimposed on the plot are the
789 confidence ellipses for categorical variables: deforested soils (orange circles), low-DBD
790 intact mangrove soils (grey squares) and high-DBD intact mangrove soils (black triangles).

791

792 **Figure 3**. Concentrations of DOC in surface water at 8 stations along the shores of the intact
793 and deforested mangrove areas.

794

795 **Figure 4.** Soil properties (bulk density, water, carbon and nitrogen contents) with cumulative
796 mass in intact and deforested mangrove soils. Insets contain soil carbon ($\delta^{13}C$) and nitrogen
797 ($\delta^{15}N$) stable isotopes with cumulative mass in a low-DBD intact and a deforested mangrove
798 soil. The line at 14 g cm^{-2} indicates the separation between the upper and bottom reference
799 soil mass layers.

800

801 **Figure 5.** Excess ^{210}Pb specific activity profiles with cumulative mass in intact (a) and
802 deforested mangrove soils (b). The filled area illustrates excess ^{210}Pb inventories.

803

804 **Figure 6.** Total ecosystem C stocks of intact and deforested mangrove forests of Tsimipaika
805 Bay, Madagascar. C stocks to 1 m have been corrected for shortening during coring as
806 described in the Methods and should be considered apparent C stocks.

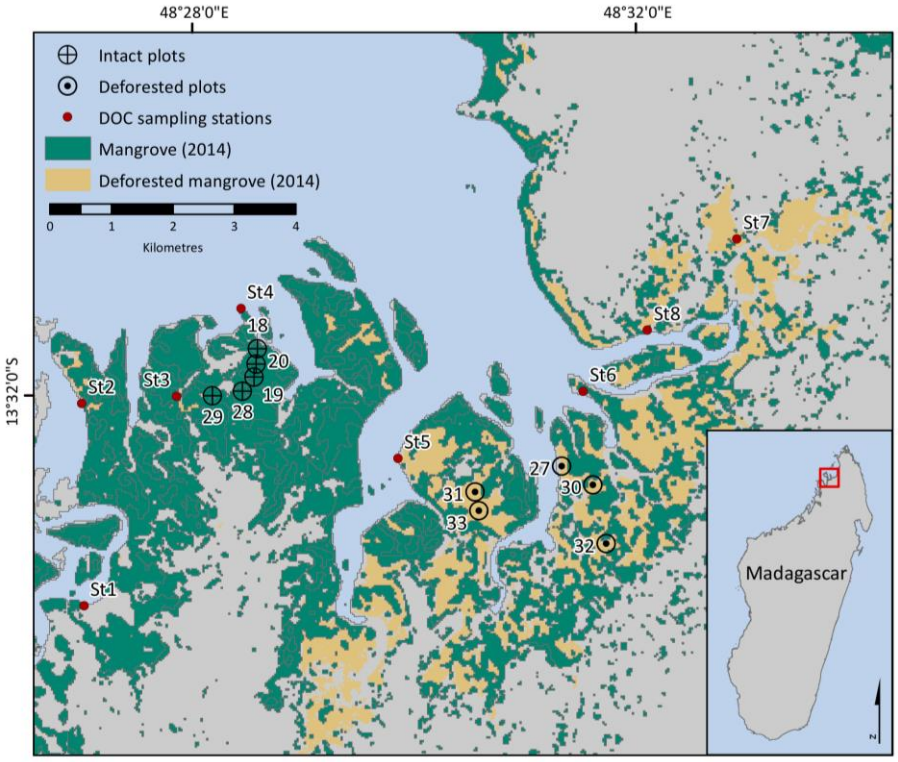

Figure 1

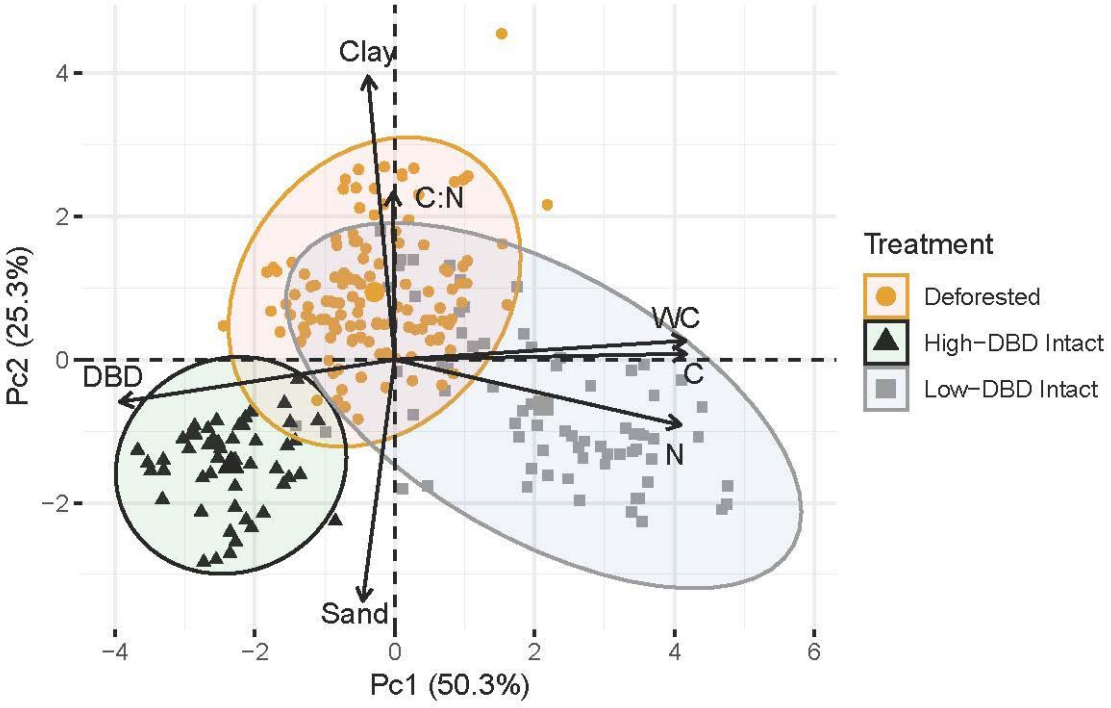

Figure 2

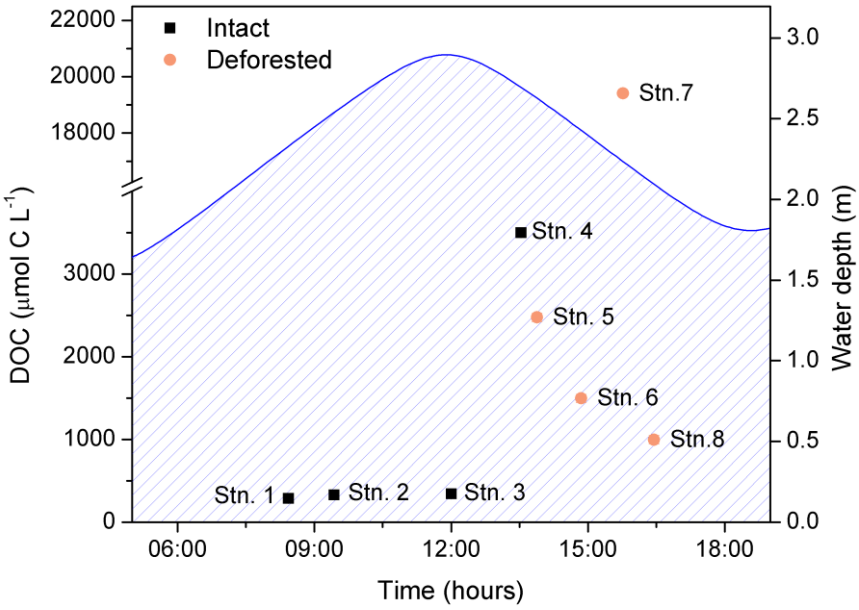

812

813 Figure 3

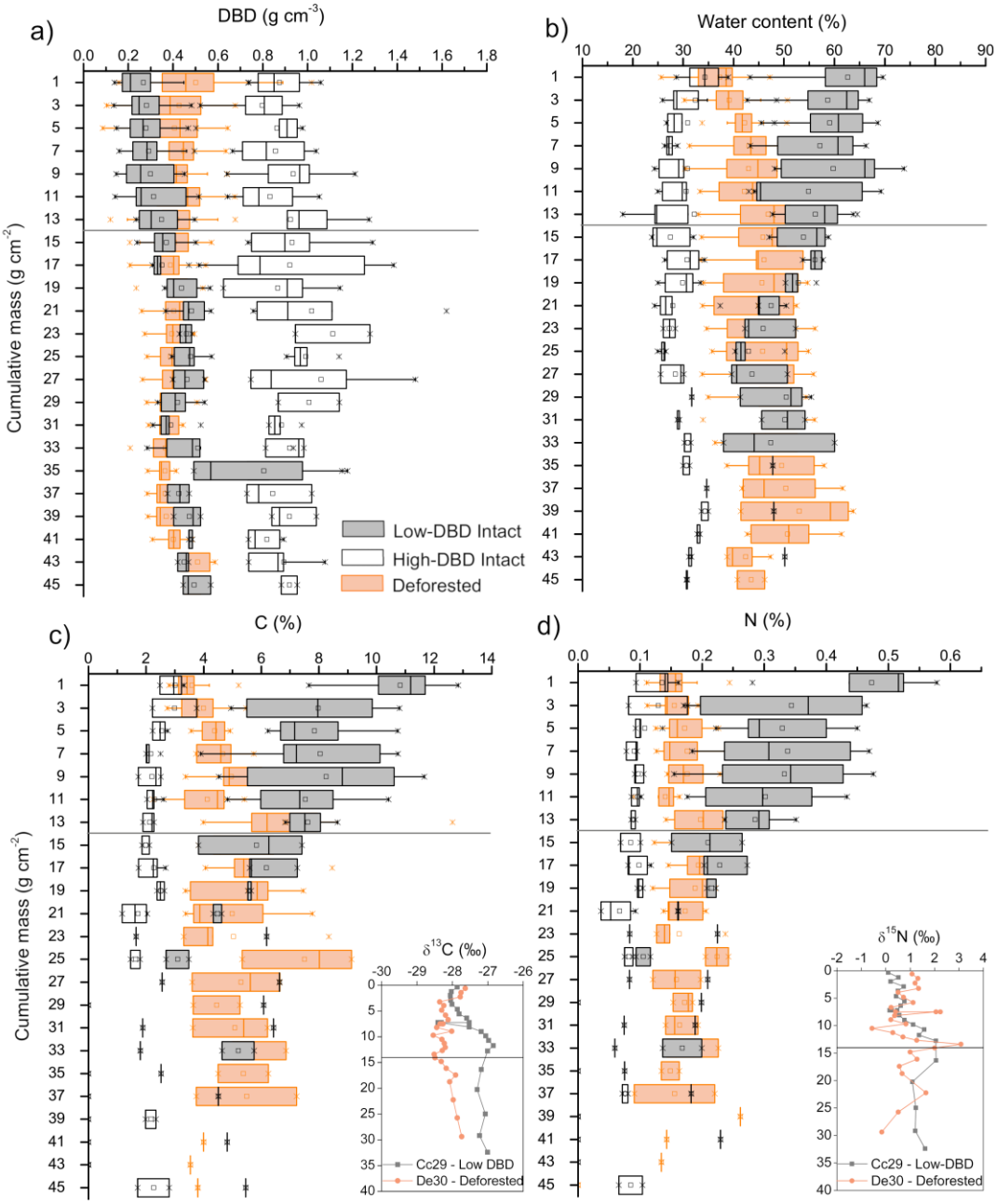

Figure 4

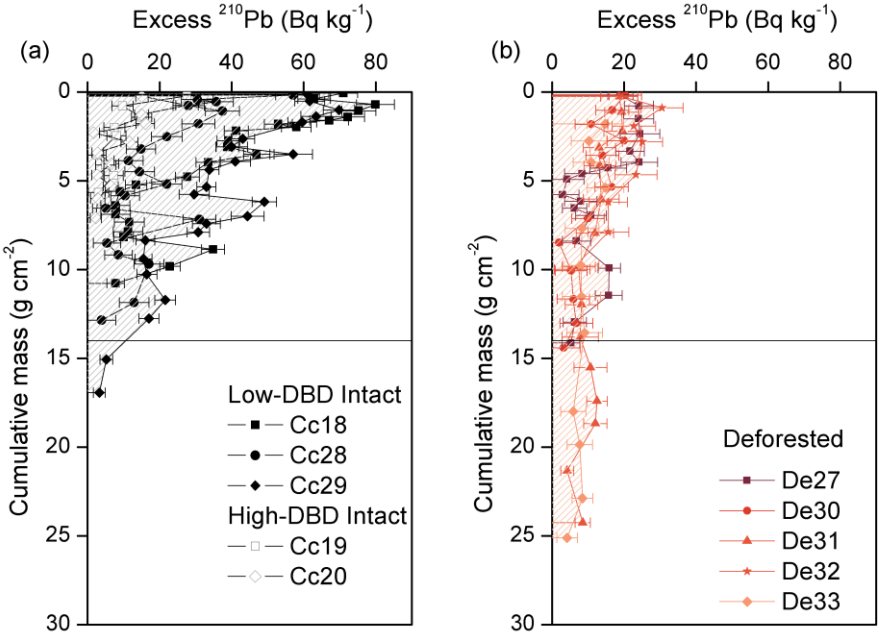

Figure 5

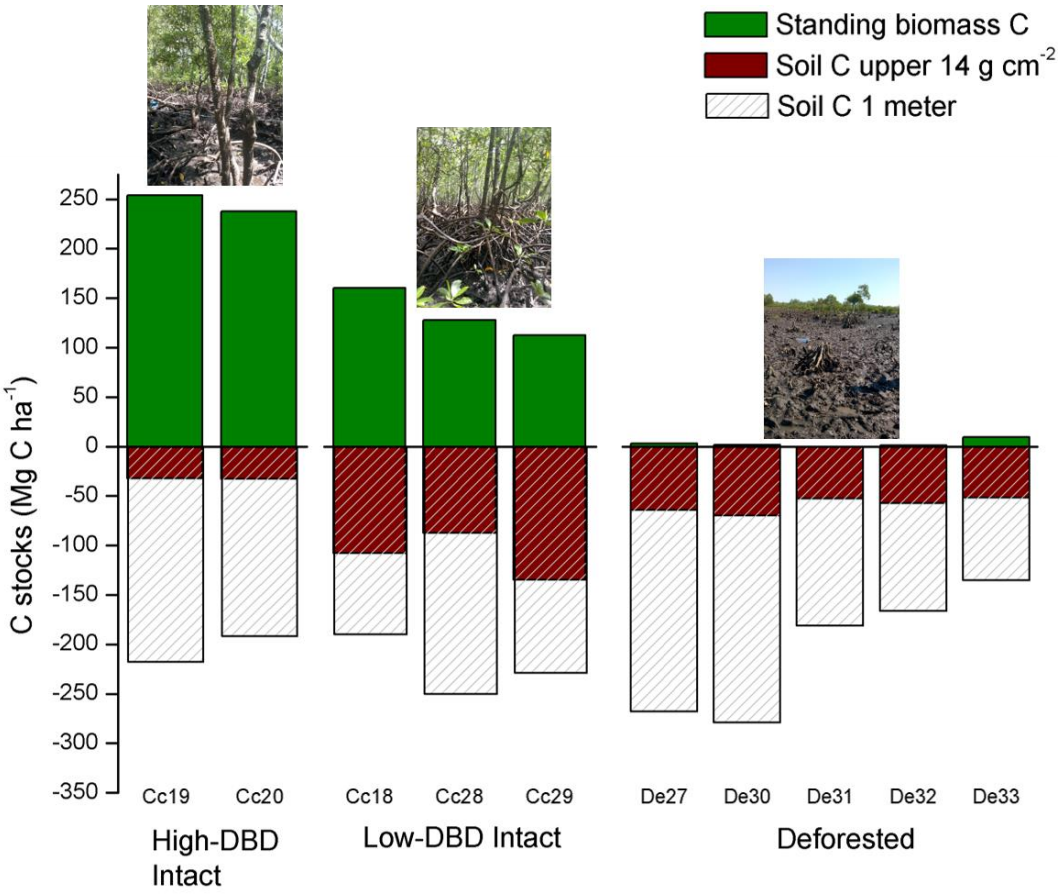

Figure 6